SAND2014-19697R

SAND20XX-XXXXR
LDRD PROJECT NUMBER: 173869
LDRD PROJECT TITLE: Structural Changes of Self-Assembled Leas Sulfide, Polystyrene Thin Films Under Extreme Pressure Using in-situ High Pressure Small Angle X-ray Scattering
PROJECT TEAM MEMBERS: Joshua Hill

ABSTRACT:

Polymer nanocomposite films consisting of polystyrene (PS) and lead sulfide (PbS) quantum dots, as well as pure PbS quantum dot films were synthesized for the purpose of investigating the pressure directed assembly (PDA) of the nanomaterials and the interactions of polystyrene and the quantum dot superlattice under pressure. Samples were compressed using a diamond anvil cell (DAC) to pressures greater than 15 GPa and studied using x-ray synchrotron radiation in order to show the changes in the d-spacing of the superlattice with respect to pressure. Absorption characteristics were investigated with ultraviolet visible spectroscopy (UV/Vis), while structure and long range ordering of the lattice were studied using small angle x-ray scattering (SAXS) as well as grazing incidence small angle scattering (GISAXS). Particle size was examined with transmission electron microscopy (TEM). These inquiries into size, structure, and interactions were performed in order to gain a baseline understanding of the interplay between nanoparticles and a simple polymer in a composite system and how the composite systems can be composed in future experiments.

1. INTRODUCTION:

Semiconductors are materials with a valence and conduction band that allow an electron to be excited from the valence band to the conduction band upon the interaction of a photon with energy above the band-gap of the material, leaving behind a ‘hole’ in the valence band. The excited electron that escaped from the valence band then relaxes back to the valence band, and releases a photon of less energy than the original incident photon; this process is called radiative recombination.

As the electron relaxes back to the valence band, non-radiative recombination can also occur which can be the result of 1) an electron, hole pair, or exciton, trapped in a defect located in the material or 2) non-radiative Auger recombination at the surface of the material, the process by which an exciton recombines without the release of light, but rather an electron.[1]

The distance of the exciton, as well as the wavelength or energy of the emitted light from radioactive recombination is characteristic to each bulk semiconductor. However, as the size of the bulk semiconductor material decreases, quantum effects begin to dominate the traditional

Sandia National Laboratories is a multi-program laboratory managed and operated by Sandia Corporation, a wholly owned subsidiary of Lockheed Martin Corporation, for the U.S. Department of Energy’s National Nuclear Security Administration under contract DE-AC04-94AL85000

physics. One particularly well known effect is quantum confinement, which is a result of when a physical dimension of the bulk semiconducting material is decreased to the point of being smaller than an exciton generating from the material's interaction with light. This quantum confinement results in various material properties including an increase in the band gap, as well as tunable photon absorption and emission.[2]

A phenomenon of particular interest is when the size of the bulk semiconductor is reduced in all three dimensions so that the exciton radius, commonly referred to as the Bohr radius, is larger than the actual size of the semiconducting particle. This results in three dimensional confinement of the exciton and the resulting nanoparticle is referred to as a quantum dot. The effective mass model, shown in equation 1.1, proposed by L.E. Brus in 1986 does an excellent job of quantifying the quantum confinement phenomenon.[3]

$$E^* = \frac{hc}{\lambda} = E_g^{bulk} + \frac{\hbar^2\pi^2}{2er^2}\left(\frac{1}{m_e m_0} + \frac{1}{m_h m_0}\right) - \frac{1.8e}{4\pi\varepsilon\varepsilon_0 r} - \frac{0.124e^3}{\hbar^2(4\pi\varepsilon\varepsilon_0)^2}\left(\frac{1}{m_e m_0} + \frac{1}{m_h m_0}\right)^{-1}$$

Equation 1.1

Where: E* = Increased band gap of the particle
$E_{g,\,bulk}$ - bulk band gap (eV)
h - Plank's constant (h=6.626x10-34 J·s)
c – Speed of light in a vacuum (2.98x108 m/s)
λ – Wavelength of the light
r – Radius of the particle
e - Charge on the electron (1.602x10-19 C)
m_e - Electron effective mass of the material
m_0 - Free electron mass (9.110x10-31 kg)
m_h - Hole effective mass of the material (cm^{-1})
ε - Relative permittivity
ε_0 - Permittivity of free space (8.854 x10-14 F)

The second term on the right hand side (RHS) of the equation is consistent with the particle in a box quantum confinement model proposed by Erwin Schrodinger, where a particle of mass, m, confined in an infinite potential square well of length, L, will form standing waves of varying frequencies. This second term on the RHS of the equation shows how a high electron confinement due to small size alters the effective mass of an electron compared to a bulk material. The third term on the right hand side accounts for the interaction of a positive hole and a negative electron which results in the Coulombic attraction between electrons and holes lowering the energy For more information on see Brus' original work.[3]

Nanocrystalline semiconductors were first discovered in the early 1980's by Alexei Ekimov, a Russian solid state physicist, who was working with microscopic CuCl semiconductors grown in a transparent dielectric matrix.[4] Ekimov found that when silicate glass, doped with bulk copper and chlorine, is heated to a sufficiently high temperature, the characteristic exciton-absorption peak for the CuCl semiconductor appears in the transparent region of the silicate spectrum. It was found that CuCl forms as a result of phase decomposition of their bulk counterparts

supersaturated in the silicate matrix. Soon after Ekimov's work with CuCl was published, Louis E. Brus synthesized CdS quantum dots in an aqueous colloidal solution.[5] However the use of quantum dots goes back much further in history. A process for synthesizing colloidal PbS nanocrystals was developed more than 2000 years ago using abundant, low-cost natural materials such as PbO, $Ca(OH)_2$ and water. Romans and Greeks used the materials to form a dye used to blacken the color of hair and provide a more youthful appearance.[6]

One-pot colloidal solution phase synthesis techniques for producing monodisperse nanoparticles suspended in solution (colloid) have been a research topic of considerable importance in the past due to the relative ease of synthesis and low cost in comparison to vapor phase synthesis methods.. The process of colloidal synthesis of nanoparticles is understood well enough, that it is has been shown that the growth of a nanoparticle, in general, can be broken down into the following three steps; particle nucleation, Ostwald ripening of the nanoparticles in solution, and saturation, as shown in Figure 1.2.

Particle nucleation is initiated by a rapid injection of a precursor solution into a typically hot solvent, followed by the growth of larger particles at the expense of smaller ones. Ostwald ripening refers to the process by which larger particles grow larger at the expense of smaller ones, thus eradicating all particles beneath a threshold size. As additional larger particles are formed by the incorporation of smaller ones, the growth no longer occurs at such a fast rate and saturation of the final nanoparticles is reached resulting in a solution of nanoparticles suspended in a solution, assuming particle agglomeration does not occur.

Agglomeration is prevented by the use of capping ligands. Often organic surfactants, these capping ligands provide a soft buffering layer around the hard inorganic core for each particle and inhibit the tendency of nanoparticles to minimize the free energy of the surface by agglomerating. Provided agglomeration does not occur and the nanoparticles are sufficiently monodisperse, self-assembly of the particle will proceed, which allows the particles to pack into a more energetically favorable structure. Face centered cubic and body centered cubic unit cells are the most common for spherical nanoparticles.

It is noted throughout the literature that the main parameters for control of size and shape of the nanoparticles are the reaction solvent, chain length of the precursor capping ligands, reaction temperature, and concentration of the precursors. Obtaining a desired shape and size requires a careful balance of these five parameters.

When the reaction solvent and precursors are heated together to a sufficiently high temperature, the precursors decompose to form chemically active atomic and/or molecular species. These atomic and molecular components form the nanocrystals whose growth is affected by the surfactant capping ligands which not only prevent agglomeration but can encourage particle growth in certain directions.[24]

In particular, lead sulfide quantum dots can be made using an inorganic Pb precursor dissolved in solution of the capping ligand, followed by injection of a sulfur precursor. A typical reaction takes place in a three neck round bottom flask, attached to a condensing column, a Schlenk line for evacuating and back filling the reaction flask, and a heating mantle underneath attached to a heating controller. Evacuating air from the reaction chamber then back-filling with ultra-high purity (UHP) nitrogen removes components that might be dissolved in the capping ligand, Pb precursor reaction solution; such as air and water. The removal of these components provides reaction conditions more controllable for particle growth. Injection of the sulfur reactant, reaction temperature and growth time largely affects the size, shape and size distribution of the particles. Reaction quenching is a necessary method for stopping the particle growth process in a controlled manner and is vital to achieve monodispersity. Mondispersity is vital to achieve uniformity of the colloid, because emission and absorption bands are dependent on the size of the quantum dots.

Reaction quenching is done with ethanol by removing the reaction flask from the heating mantle, and adding the polar solvent into the reaction vessel to sufficiently cool and halt the growth process in addition to aiding in precipitation and washing the colloid of excess reactants. Quenching process, a wash and size selective precipitation is performed in ethanol in order to remove any unreacted, remaining precursor. The mixture of reaction solution and ethanol is centrifuged and the supernatant is removed. The remaining precipitate is then re-dispersed in an appropriate organic solvent. Usually toluene is chosen as the organic solvent due to its relatively high boiling point. To ensure the particles are roughly homogenous, the organic solvent is added to the centrifuge precipitant and sufficiently mixed so that no aggregates can be seen in the solution.

Once the washing procedure has been completed, optical characterization, UV/Vis absorption, and photoluminescence is usually carried out first. It is important to choose a solvent whose absorption of emission characteristics will not interfere with the region of the spectrum one is trying to investigate. Toluene will prevent absorption data from being seen in the 2000-2500nm region of the spectrum, so the sample was re-dispersed in tetrachloroethylene in order to obtain absorption spectra.

Preparing specimens to be studied by the transmission electron microscope (TEM) in order to view the nanoparticles is crucial as well. To do this, it is advantageous to place a drop or two of the solution on top of water in order to form a monolayer of the colloid. A TEM grid can then be dipped into the solution, breaking the film, removed and allowed to dry. The drying process is important if an ordered array is to be obtained. In order to achieve this, it is best to cover the grid so that any air movement in the area does not disturb the self-assembly of the nanoparticles while the solvent evaporates.

A similar process is used when forming films containing ordered arrays of the nanoparticles on a substrate. The substrate must first be cleaned, commonly done by sonication in ethanol. This is followed by thoroughly rinsing the substrate in acetone, followed by ethanol, and once more followed by acetone in order to remove all contaminant. After visual inspection and drying with a stream of UHP nitrogen gas and once again visually inspected the colloidal solution can then be carefully dropped onto the substrate and covered to prevent any air movement in the area from disturbing the self-assembly process.

The oxidation of the synthesized PbS forms a silvery-white powder, usually over the course of several days. To prevent this oxidation, films and solutions should be stored in a glovebox filled with an inert gas. Investigation of the dried films for an ordered structure is accomplished using SAXS.

Pressure Directed Assembly

In-situ high pressure small angle x-ray scattering (HP-SAXS) is an analytical technique that allows the investigation of structures of micrometer scale or smaller while placed under pressure, and in real time, and tracks how the material responds to large changes in pressure. With only a handful of scientific articles published on the pressure directed assembly of nanoparticles, it is a topic of recent interest in the field of nanoparticle research and is open to a wide range of experiments, such as high pressure particle sintering, or low pressure reversible compression for a wide range of materials.

Podsaidlo et al. have done high pressure diamond anvil cell (DAC) experiments using PbS nanoparticles which show an increase in the ordering of the face centered cubic structure as the pressure reaches approximately 8 GPa, the threshold pressure.[29] This increase in structural ordering is followed by a slight decrease in the order of the structure as the pressure is increased; however the PbS nanocrystals retain their preferential orientation as high as 55 GPa. This article provides the basic information about the properties of the threshold pressure, how the pure PbS quantum dots shift, and d-spacings, or the space between domains of the lattice of particles comprising larger domains of an ordered structure, commonly referred to as a superlattice, change when pressure is applied.

In another article that focused on HP-SAXS, using a DAC, Wu et al. investigated the high pressure assembly of gold nanoparticles and first proposed the concept of irreversible particle sintering above threshold pressure, which results in a three dimensional network of interconnected gold nanoparticles. [32] Wang et al. have also performed work with PbS quantum dots under high pressure to investigate the stress driven orientation and attachment of the nanoparticles.[31] Wang et al. showed that the entire resulting structure can be drastically different when performed without a hydrostatic medium, which induces a deviatoric stress resulting in the formation of nanosheets.

Taking clues from each of these notable articles, the experiments performed not only compress the nanoparticles, but incorporate polystyrene into the structure as well in order to investigate what interactions will occur when a polymer such as polystyrene is used in conjunction with PbS quantum dots. These experiments provide the platform needed to begin using conductive polymers, which will most likely be used as sensors, triggers and optoelectronic systems. Increased interdigitation will provide a higher degree of intimacy among the polymer chains. In terms of conductive polymers and optoelectronics, this could result in a more efficient means of signal transport.

Observations using SAXS and grazing incidence small angle x-ray scattering (GISAXS) have shown that provided the appropriate conditions such as molecular weight and concentration, the chains of polystyrene can be inserted between the domains in the unit cell of the superlattice of quantum dots, rather than around the superlattice. This polymer insertion between the domains can be shown by an increase in the d-spacing of the superlattice. Once polystyrene is inserted between the domains, the threshold pressure, the pressure with the lowest d-spacing where ligand interdigitation occurs, is expected to decrease. This is particularly interesting because only a certain molecular weight polymer chain of a certain concentration can insert itself between the domains of the superlattice. A decrease in superlattice domain distance would increase interplay and communication among the particles in the different domains. This decrease is superlattice domain distance can be especially useful in systems of nanoparticles such as nanogold or nanosilver where plasmon resonance, collective oscillations of electrons by incident light, occurs. As distance decreases, an increase in plasmon resonance would increase, and provide some very useful properties to those interested in such systems.

The structural properties of this phenomenon should be studied to understand the interplay of nanoparticles and polymer. A decrease in the threshold pressure is expected to occur because the domains of the superlattice will be further from each other than in a superlattice of pure PbS. This interaction of the capping ligands with the polystyrene chains in turn will advance the interdigitation of the capping ligands with each other and result in a lower threshold pressure that will be required to achieve interdigitation and particle sintering. On the other end of the spectrum, when the chains of polystyrene surround the domains of the superlattice, the threshold pressure will be lower because less force will be required for interdigitation of the capping ligands, as they will already be forced to sit close to one another.

2. SYNTHESIS AND FORMATION OF ORDERED ARRAYS OF LEAD SULFIDE NANOPARTICLES

Particle Synthesis

In order to synthesize the PbS quantum dots, a solution of the lead precursor, capping ligands, and high boiling point solvent was prepared. The lead precursor used throughout the experiments was lead oxide (PbO), and the capping ligand and high boiling point solvent was oleylamine.

Lead sulfide quantum dots were prepared according to the synthesis method provided by Hines and Scholes.[9] Once the solution of oleylamine and lead oxide was prepared in a three neck round bottom flask, the heating mantle, rubber septums and condensing column were set in place. Using a vacuum pump, the chamber was then evacuated of air while being heated to 130^{o}C. This allows the solution to degas and removes any O_2 which will not allow the reaction to proceed as desired. After about 30 minutes, the chamber was backfilled with UHP nitrogen, and evacuated again. This process was repeated four additional times to ensure an oxygen free environment for synthesis.

During this process of heating, magnetic stirring and along with degassing, the yellow solution becomes clear indicating that the PbO has become sufficiently dissolved in solution that it no longer interacts with visible light. At this point, hexamethlydislithiane in oleylamine is carefully and quickly injected into the flask to form a ratio of OA:Pb:S of 4:2:1 and the temperature is lowered to 110^{o}C. As the PbS nanoparticles nucleate and begin to grow via Ostwald ripening, the solution turns from clear to a deep brown and finally black.[7]

After reacting for 1 minute, the heating mantle is lowered from the reaction flask, and the reaction flask is filled with a solution of ethanol in order to quickly quench the growth process. The solution is then centrifuged in a solution of 90 volume % ethanol and 10 volume % PbS organic solution at 6,000rpm for 7 minutes. The solution is decanted, and the process repeated two additional times to ensure the quantum dots are free of any excess organics, which would interfere with the self-assembly of the superlattice structure of the quantum dots. The precipitate is then collected by redispersing in a small amount of toluene and allowed to rest for about 72 hours to ensure the size narrowing regime is allowed to proceed.[9] The solution is then adjusted to the desired concentration in toluene.

In order to form the self-assembled films, PbS in toluene was used with a concentration of 100mg/mL. A 50μL drop of the solution is then carefully dropped onto a silicon wafer cleaned by sonication in acetone and three alternating washes of acetone and ethanol followed by drying in a stream of UHP nitrogen. The wafer with the drop of solution was carefully covered so that air movement in the room would not interfere with the evaporation of the solution and self-assembly of the superlattice. In the cases where polystyrene is used to form a nanocomposite film, the appropriate amount of polystyrene was added to the PbS, toluene solution, sonicated, and drop cast onto a silicon wafer. In order to proceed with experimentation, confirmation of the self-assembled superlattice was necessary. This was performed by obtaining a small angle x-ray diffraction (SAXRD) pattern of the wafer with the dried drop cast film. If the SAXRD pattern showed that the superlattice had self-assembled, as seen in Figure 3.1, the film could be used for grazing incidence small angle scattering and pressure directed assembly.

Analysis Preparation

Small Angle X-ray Scattering

To prepare nanoparticle quantum dots for small angle x-ray scattering, a small drop (~50μL) of the colloidal PbS in toluene is carefully placed on a clean silicon wafer, and allowed to dry, this process is commonly called drop casting.

Transmission Electron Microscopy

Because specimen integrity is vital for further investigation, great care must be taken when undertaking the steps required to prepare a specimen for high resolution TEM imaging. TEM specimens from the PbS and PbS-PS colloidal solutions were prepared by filling a Petri dish with deionized (DI)water and placing a drop of the toluene colloid solution on the surface so that a monolayer of the colloidal forms on top of the water. A carbon coated holey copper grid was then plunged in the solution, removed and carefully covered so that any air currents do not interfere with the self-assembly of the colloid before the solvent evaporates. In order to prepare TEM specimens of the samples after the PDA, a small amount of the sample is removed from the diamond anvil cell with a cleaned needle tip. A drop of toluene is then carefully removed from a pipette, allowed to contact the needle tip and fall on the carbon coated holey copper grid. The TEM grid is then covered, again to prevent any air movement to interfere with the self-assembly of the sample before the solvent evaporates.

Grazing Incidence Small Angle Scattering
In order to further understand how the nanoparticles arrange on a substrate, grazing incidence small angle scattering (GISAXS) is employed to investigate the superlattice structure of the nanoparticles on the surface, buried within the film, and at the substrate film interface. The GISAXS instrument uses a a shallow beam angle of about 0.15^{o} with respect to the horizontal sample. With this sahllow beam angle the superlattice can be analyzed in the range from nanometers to micrometers. These experiments were performed at Cornell's CHESS Lab's D1 line; the synchrotron radiation provides an excellent photon source for investigating films of nanoparticles on the surface of a substrate due to its high resolution and x-ray flux.

Pressure Directed Assembly
The pressure directed assembly of the nanoparticles is performed in a diamond anvil cell by placing a small amount of the PbS film sample in the gasket of the cell chamber, along with silicon oil as a pressure-transmitting fluid and a small grain of ruby powder for pressure calibration as shown in Figure 3.15. The diamond anvil cell is then constructed and used for experimentation.

Due to the extremely high resolution needed to record Angstrom size changes in geometry of the superlattice, synchrotron x-ray radiation is required to investigate the change in d-spacing as the pressure is changed. This was performed at the B1 line at the Cornell High Energy Synchrotron Source at Cornell University.

3. RESULTS AND DISCUSSION

A variety of techniques can be used for characterization of the nanocrystalline PbS quantum dots. All techniques, however, employ the use of electromagnetic radiation of wavelengths shorter than visible light or electrons to interrogate the sample. This is because the wavelength of visible light is too large to probe between individual nanoparticles, therefore no information can be obtained.

Absorption Spectroscopy
Ultraviolet visible (UV/Vis) absorption is a useful tool for the characterization of quantum dots in solution, as well as indirectly investigating particle size and particle distribution because the short wavelengths involved. The goal of synthesizing PbS with a small size distribution, or monodisperse, can be first investigated through UV/Vis. The more monodisperse the nanoparticles in the solution, the more uniform the properties of absorption, emission, and the more readily ordered structures will self-assemble.

The excitation of the quantum dots by a particular wavelength of light, which is determined by particle size, results in the absorption of a particular wavelength of light that is tunable according to the size of the particles. This absorption phenomenon which presents itself as a peak in the absorption spectrum is referred to as the first absorption edge. The full width at half maximum of the absorption peak is an indication of the monodispersity of the particles, as more monodisperse sample will have a smaller full width at half maximum. The absorption spectra of the PbS quantum dots used throughput the rest of the experimentation are presented in Figure 3.2. It is crucial to note that the spectra are nearly identical with only 1 nm separating the first absorption peaks. This indicates that even though the nanoparticles were made in separate batches, they are nearly identical. This will be very important for comparing, and correlating data from other techniques such as high pressure small angle scattering and grazing incidence small angle scattering.

Small Angle X-ray Scattering

The wafer with the dried PbS sample is analyzed using Small Angle X-ray Scattering (SAXS) to investigate the resulting superlattice formation. As presented in Figure 3.3, the two samples chosen for further analysis clearly display the peaks that correspond to the [111], [311] and [420] planes without much variation in d-spacing. It is critical to obtain a good SAXS spectrum as a starting point before further experimentation and analysis to ensure that the sample is well ordered. Being able to clearly resolve a minimum of three peaks is also important, as this helps to identify the visible lattice planes in the sample, referred to as indexing the pattern. It must be noted, that these peaks do not correspond to the structure of PbS in its crystalline bulk form or even in the nanocrystalline from. These spectra correspond to the superlattice composed of domains of ordered arrays of nanocrystalline PbS.

Transmission Electron Microscopy

Figure 3.4 shows a micrograph at 20,000X magnification of pure PbS. Here, ordered arrays of the nanocrystalline semiconductor can be seen in the various islands. A closer look from 100,000X magnification (Figure 3.5) shows a more detailed view of the order that the quantum dots arrange themselves in order to minimize the free energy among the particles. An even closer view at 300,000X magnification in Figure 3.6 shows the amazing uniformity of the ordered array as well as the lattice fringes of the particles comprising the quantum dots.

Grazing Incidence Small Angle Scattering

The GISAXS data obtained for a film of pure PbS at 1mg/mL (Figure 3.7) shows that the base layer of the film forms a superlattice that orients itself with respect to the substrate very well, and loses order with additional vertical stacking. This can be seen by viewing the number of rings that are present at the lower incidence angles such as 0.15^{o} and 0.25^{o}.

However, at steeper angles such as 0.40^{o} and 0.50^{o}, more of the interface of the silicon substrate and the PbS film is interrogated. At these larger angles we can see discreet dots start to appear. Each dot describes a particular orientation of the superlattice formed on the substrate. The scattering obtained from the surface shows these discreet dots rather than the ring patterns because when the nanocrystals are randomly oriented, the discreet dot patterns are essentially spun around the central beam axis and a powder ring pattern is formed. This information tells us that in order to attain films with the most ordered structure of PbS nanocrystals, the film must not exceed a certain height with the current drop casting technique. This behavior can be likened to that of children's building blocks being randomly laid out on a surface. The initial layer will show more order than additional layers of blocks on top of blocks.

The spectrum has been indexed and corresponds nicely with the traditional face centered cubic pattern (Figure 3.8). These spectra show that as the polystyrene is added, more rotational freedom of the superlattice domain is allowed because the increase in concentration of polystyrene is accompanied by an increase in the amount of powder diffraction rings. These powder diffraction rings are not only seen near the surface of the film at low incidence angles, but also near the surface at the higher incidence angles of 0.40^{o} and 0.50^{o}. Because it was determined from SAXS that 820 g mol^{-1} polystyrene at concentrations as low as 5wt% inserts itself between the domains of the superlattice, we can see that this also causes the superlattice domains to rotate out of the preferred order that is obtained with additional amount of 820 g mol^{-1} polystyrene. The same set of data was then collected for PbS with 18,100 g mol^{-1} polystyrene in various concentrations and angles as shown in Figure 3.10. The SAXS data showed that this molecular weight of polystyrene surrounds the domains of the superlattice, decreasing the d-spacing of the superlattice.

The GISAXS data of PbS with 18,100 g mol^{-1} polystryrene is similar to the 820 g mol^{-1} PbS-PS films but with an increased amount of rotational freedom in the presence of increasing amounts of the polymer. However, between the weight percentages of 75% and 90%, there is a decreased amount of the powder ring diffraction pattern near the [111] and [311] planes indicating that in this case, less rotational freedom of the superlattice domains is allowed and a more ordered superlattice is obtained. The final molecular weight of polystyrene used in these GISAXS experiments was 97,400 g mol^{-1}. Again the surface of the film shows little order with the powder ring diffraction pattern dominating the spectrum at the lower incidence angles as shown in Figure 3.11. Even at 5wt%, and near the interface of the film and the substrate, a large degree of rotational freedom is observed. However, the pattern obtained from the 10wt% and 25wt% samples shows a change to a more ordered superlattice along the [111], [220] planes. After this point, an increased amount of powder ring patterns is seen, showing an increased amount of rotational freedom along all planes. This shows that the "sweet spot" for obtaining the most order in the 97,400g mol^{-1} PbS-PS films is between the 10 and 25wt% polystyrene. Figures 3.8-3.10 show the GISAXS patterns obtained for the various PbS-PS films at 5, 10 and 25wt%.

For 5wt% films it is clear that less in-plane ordering of the superlattices is obtained with increasing molecular weight of the polystyrene. Small angle x-ray scattering showed that increased molecular weight polystyrene resulted in decreased d-spacing as the polymer chains surround the domains of the superlattice. This phenomenon of surrounding the domains will result in increased stress in the superlattice in comparison to the pure PbS superlattice. This increase in stress in the superlattice then results in decreased order, as the domains are not allowed to position as freely and obtain the desired order as in the pure PbS superlattice.

The various polystyrene molecular weights at 10wt% show a similar trend, with an increased amount of powder ring diffraction patterns with increasing polystyrene molecular weight. However, at 25wt% and angles of 0.40^{o} and 0.50^{o}, there is a decrease in the powder ring diffraction pattern between 18,100 and 97,400 g mol^{-1} polystyrene. This shows that near the interface of the film and the substrate, there is another ‘sweet spot’ for obtaining order between 18,100 and 97,400 g mol^{-1} polystyrene at 25wt%.

Pressure Directed Assembly

In situ XRD spectra were collected at various pressures for both pure and composite samples in order to determine changes in the d-spacing. The DAC is setup to allow spectra to be collected after the pressure applied to the PbS sample has been changed. Synchrotron x-ray radiation is necessary because it provides a well-focused beam perfectly suited for the sample chamber of the DAC. The sample of pure PbS drop cast onto a silicon substrate was first compressed and analyzed using the synchrotron source. The raw data of the small angle scattering for the pure film of PbS nanoparticles is shown in Figure 3.16.

It can be seen that the discreet spots, which indicate order over various planes, that are present at ambient pressure lose their distinct shape and become smeared around the ring. This data shows that as the pressure in increased, the nanoparticles in the superlattice exhibit an increase in rotational freedom with respect to the substrate, and overall superlattice order decreases with increased pressure. Integrating over 2-theta provides the spectrum that is easier to work with and make comparisons between samples. Figure 3.17 shows the integrated curves for the sample under multiple pressures and the resulting d-spacing of the [111] plane. The spectra show that upon compression, there is a gradual decrease in the d-spacing of the [111] plane up to about 6.90 GPa and subsequent expansion of the d-spacing of the [111] plane after 6.90 GPa. Once the pressure is released, the superlattice returns to within 0.03 Å of the original value. This behavior is typical of a system of nanoparticles under pressure.[32]

The sample of PbS mixed with 25wt% 820 g mol^{-1} polystyrene was then analyzed. Again, the raw HP-SAXS spectra (Figure 3.18) show the increase in the rotational freedom of the superlattice domains from 0 GPa to 5.27 GPa, by the evidence of the blurred dots around the ring. However, from 5.27 GPa, past the threshold pressure of 6.64 GPa, up to 7.22 GPa, the superlattice appears to have gained some order as the blurred dots become slightly more defined. The SAXS overlay, Figure 3.19, is difficult to analyze, as the peaks are not well defined as the pressure is increased. However, the take away from this analysis is the threshold pressure of 6.64 GPa. With a threshold pressure of 6.64 GPa for PbS with 25wt% 820 g mol^{-1} polystyrene, the hypothesis of decreasing threshold pressure with increasing molecular weight can be tested.

The raw HP-SAXS data of PbS mixed with 25wt% 18,000 g mol^{-1} polystyrene (Figure 3.20) shows an impressive amount of order present in the superlattice, as shown by the number of dots displayed around the ring. However, it can also be seen that there is a significant amount of rotational freedom among the domains of the superlattice.

However, once the pressure is increased, the rotational freedom becomes much less prevalent, and the overall order appears to slightly decrease, but is well maintained passed the threshold pressure of 6.20 GPa. This sample of PbS quantum dots mixed with 25wt% 18,000 g mol^{-1} polystyrene is a very robust sample and perhaps the kind best suited for beginning to explore more uses of the composite superlattice nanomaterial due to its readiness to form ordered arrays with relative ease. Unlike the other HP-SAXS spectra overlay, the data for PbS-25wt%-18,100 g mol^{-1} polystyrene (Figure 3.21) displays a split [111] peak at ambient pressure which returns to a single peak upon compression. This is possibly due to the amount to rotational freedom seen in the raw data that disappears as the compression is initiated.

As the molecular weight of the polystyrene is increased to 97,400 g mol^{-1}, it is again seen that the discreet spots that correlate to superlattice order become less defined with increasing pressure (Figure 3.22). The HP-SAXS overlays (Figure 3.23), show the typical behavior of the composite nanomaterial under compression and release with a threshold pressure of 5.58 GPa. The threshold pressures and d-spacings collected with the various molecular weights of polystyrene helps to paint the picture of the entire system and how the polystyrene affects the pure PbS quantum dot superlattices.

Figure 3.24 shows how the polystyrene will either insert itself between the domains of the superlattice, as in the case PbS and 25wt% 820 g mol^{-1} polystyrene, or will wrap around the domains resulting in a smaller d-spacing. In Figure 3.25, we see the general trend of threshold pressure with increasing molecular weight of polystyrene. This helps to support the hypothesis that the threshold pressure will decrease with increasing molecular weight of polystyrene. However, this data cannot conclude that the decreasing threshold pressure is caused by decreased van der Waal attractions between the domains of the superlattice, or momentary interactions due to short lived small electrical attractions and repulsions between the capping ligands of the superlattice domains.

4. ANTICIPATED IMPACT:

The anticipated impact of these experiments can be considered far reaching for the further understanding of nanoparticle physics and nanoparticle interactions with polymeric materials. Using the interactions of PbS with polystyrene of various weight percentages and densities can be used as a template for how to anticipate the interplay of the ligand capped nanoparticles in the neighborhood of 5nm in diameter with nonpolar polymers; we can began to understand these binary system in further detail. Details about the film synthesis and evolution with respect to airflow, concentration, and substrate surface can be further understood and how each of these aspects influences the short and long range order of the forming superlattice needs to be investigated. With this knowledge, science can move forward to experiment with nanoparticle-polymer superlattices of more practical use, like superlattices that contain flexible or conductive polymers with potential use in a number of optoelectronic devices.

Now that a degree of information about the formation of long range Pb- polystyrene superlattice order on silicon substrates is known, it will be more amenable to perform these experiments with a variety of materials, such as block copolymers, azoles, and thiophene. Additionally, other quantum dots can be employed. Although PbS has a wide range of exciton and emission in the infrared, other nanocrystalline semiconductors that act in the visible and ultraviolet can be employed. This will allow for optoelectronic devices such as sensor or transmitters to work in a broader region of the electromagnetic spectrum. Furthermore, the experiments do not have to be limited to quantum dots, but other nanoparticles can be employed as well.

As modern materials are tailored for the needs they must meet, so can nanoparticles be utilized in ways according to the required need. For example, gold or silver nanoparticles can be used to achieve plasmon resonance. Or in a system where there is a need for magnetism, iron oxide can be used. The experiments that have been covered in this article represent only a small number of the possible experiments that could have been performed. A greater range of polystyrene densities, or differently sized PbS nanoparticles could have been studied, more than likely with results differing from the ones observed in this set of experiments. The limit for ordered superlattice nanostructures is only limited by the imagination and extent of knowledge of those working with the materials, and will be well utilized in the future of nanotechnology. Moreover, the experiments that use a diamond anvil cell represent some of the most cutting edge and exotic research that has been performed on nanoparticles. This science has profound and potentially far reaching impacts.

The knowledge gained from HP-SAXS can provide insight on how physical and external phenomena can influence the structure and behavior of nanoparticles and the corresponding superlattice. Although the pressures used in the experiments are much higher than what is typically used in an industrial setting, the data can still be used to understand how the nanoparticle superlattice on or in a substrate can be studied and influenced in industrial forming processes such as rolling, stamping, bending, or shearing. The experiments performed using the diamond anvil cell are relatively new techniques in the study of nanomaterials and its true potential has yet to be realized. These experiments will provide many useful and insightful looks into how nanomaterial systems can be further understood and studied.

5. CONCLUSION

Lead sulfide nanocrystalline semiconductors, or quantum dots, were synthesized for the purpose of analyzing the properties of ordered superlattice arrays of the pure nanocrystals and nanocrystalline/polystyrene composites. These self-arranged ordered materials were characterized using x-ray scattering, absorption spectroscopy and electron microscopy.

The materials were then subjected to extremely high pressures and interrogated using x-ray synchrotron radiation to observe structural changes. It was observed that a certain molecular weight of polystyrene allowed the chains of the polymer to insert themselves between the domains of the quantum dot superlattice and effectively increase the d-spacing of the superlattice. It was also observed that the molecular weight of the polystyrene impacted the threshold pressure of the superlattice, and that higher molecular weight chains of the polymer in contact with the quantum dot superlattice resulted in lower threshold pressures.

This lowering of the threshold pressure is believed to be caused by the chains of the polymer forcing the domains of the superlattice to align closer, therefore less force is needed to reach the point where the capping ligands become interdigiated and the d-spacings begin to increase with increasing pressure.

List of Figures

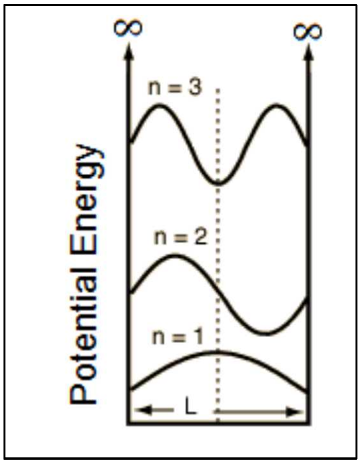

$$E_n = \frac{n^2 \hbar^2 \pi^2}{2mL^2}$$

Figure 1.1 - Quantum confinement model proposed by Erwin Schrödinger

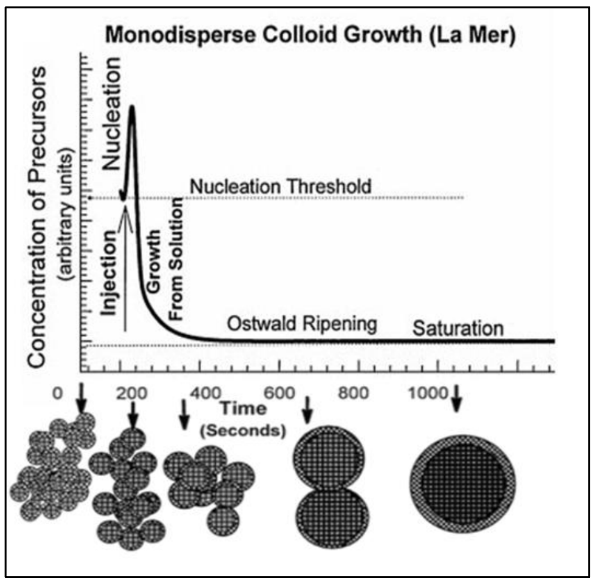

Figure 1.2 - Particle nucleation and growth model[7]

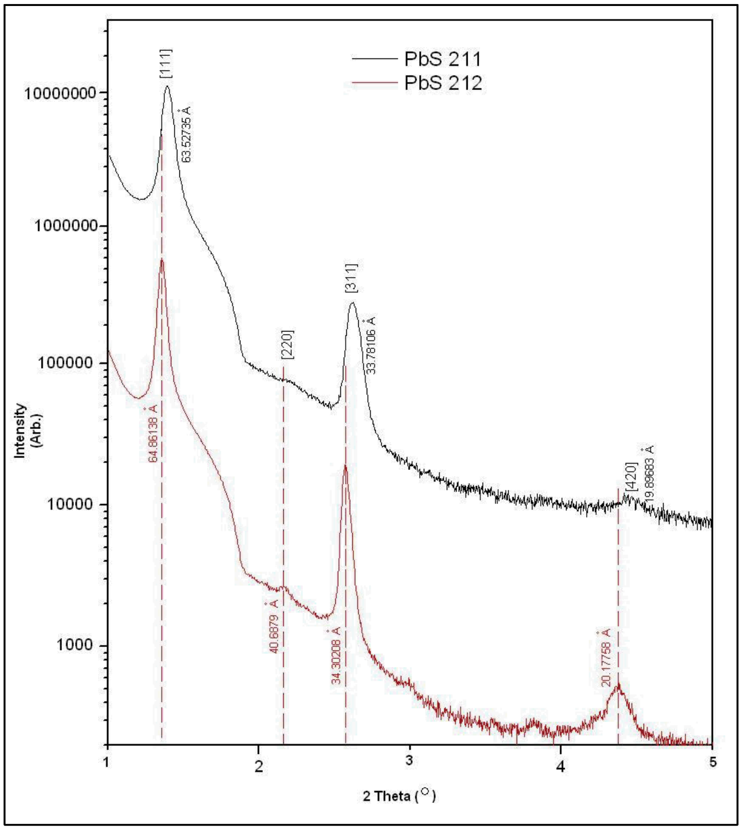

Figure 3.1- Small angle X-ray Scattering of Pure PbS quantum dots

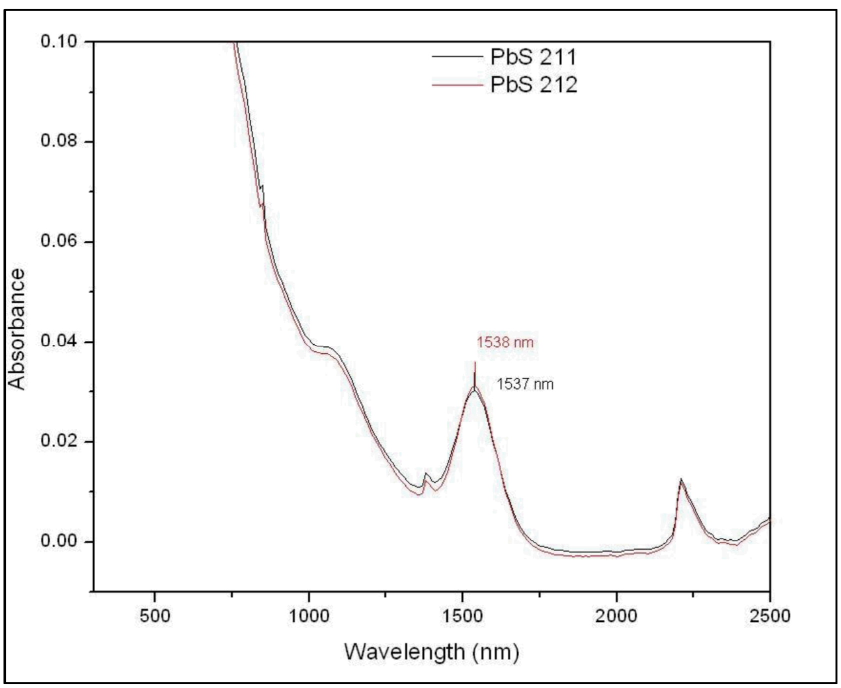

Figure 3.2 - UV/Vis spectra of pure PbS quantum dots

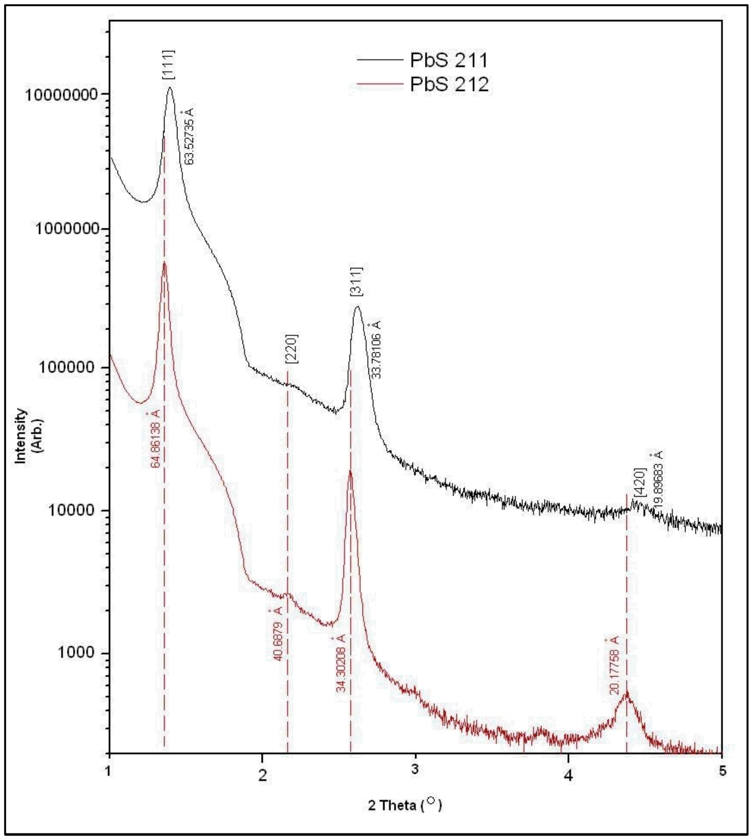

Figure 3.3 - Small angle X-ray Scattering of Pure PbS quantum dots.

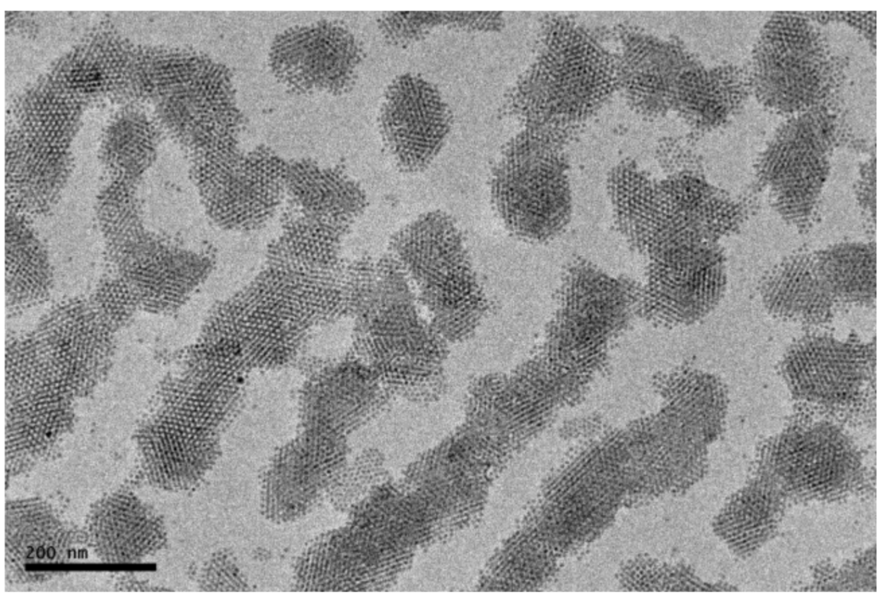

Figure 3.4 - Transmission Electron Microscope image of pure PbS nanocrystals at 20,000X magnification

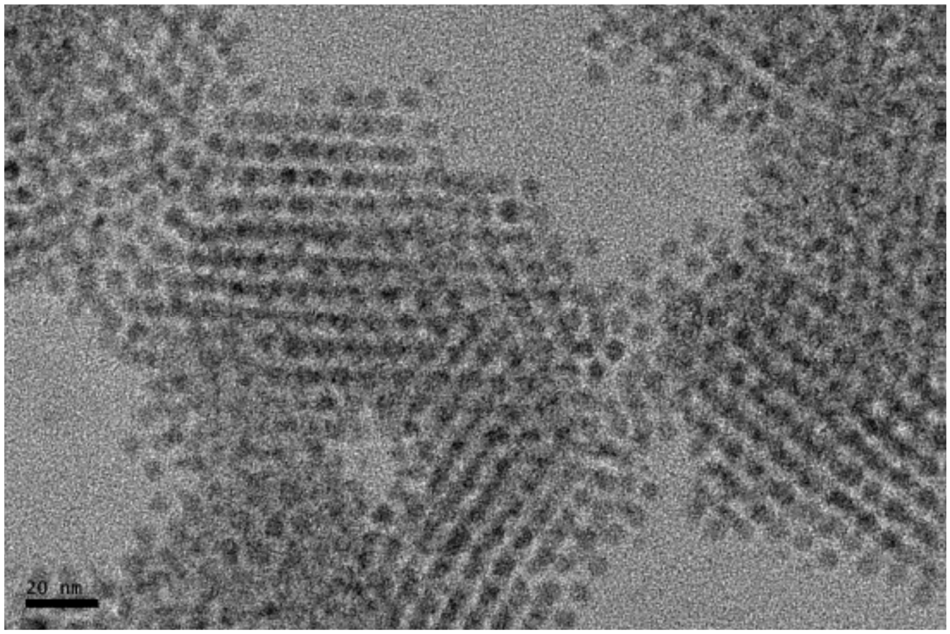

Figure 3.5 - Transmission Electron Micrograph of pure PbS quantum dots at 100,000X magnification

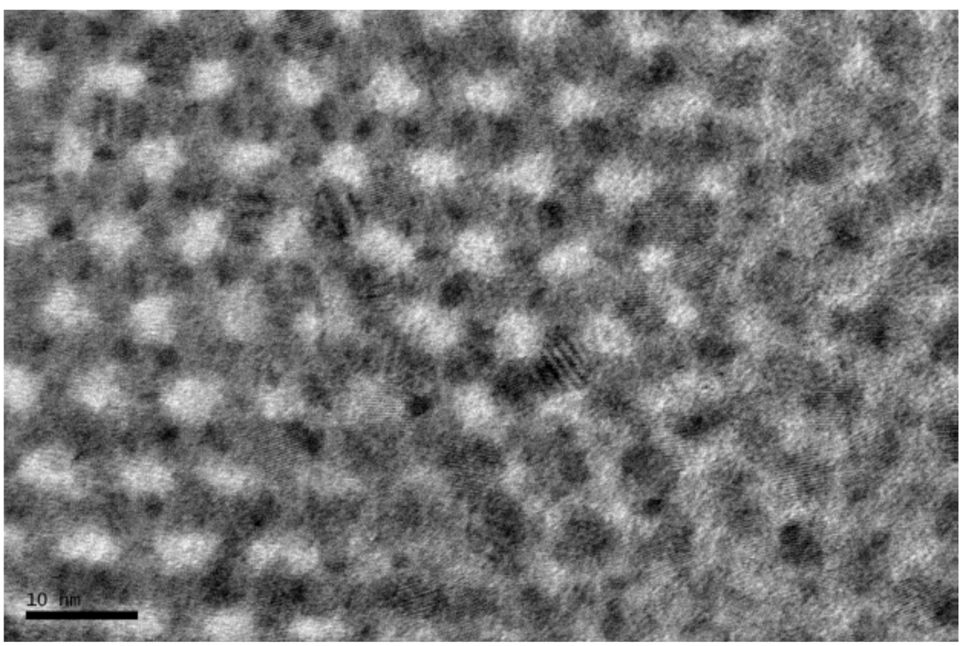

Figure 3.6 - Transmission Electron Micrograph of pure PbS 300,000X magnification

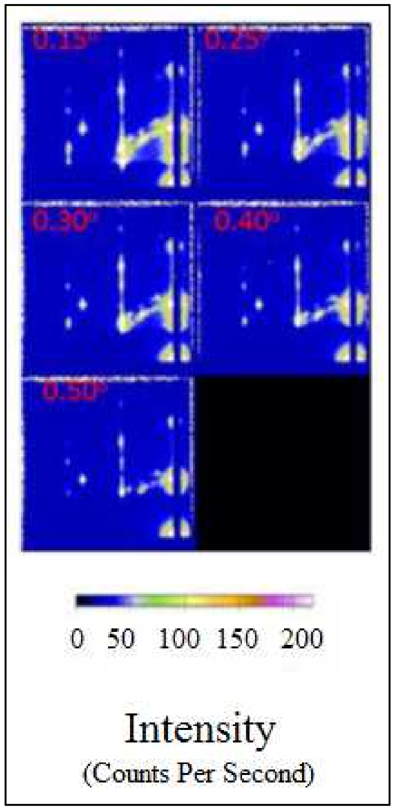

Figure 3.7 - GISAXS spectra of pure PbS at various incident angles

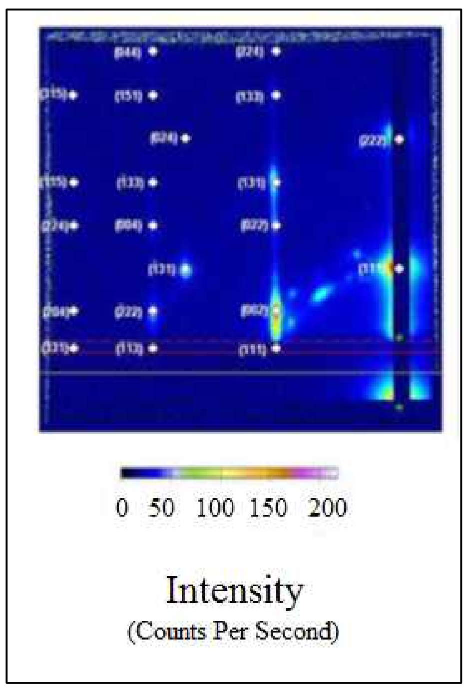

Figure 3.8 - Indexed GISAXS spectrum of Pure PbS, (Face Centered Cubic)

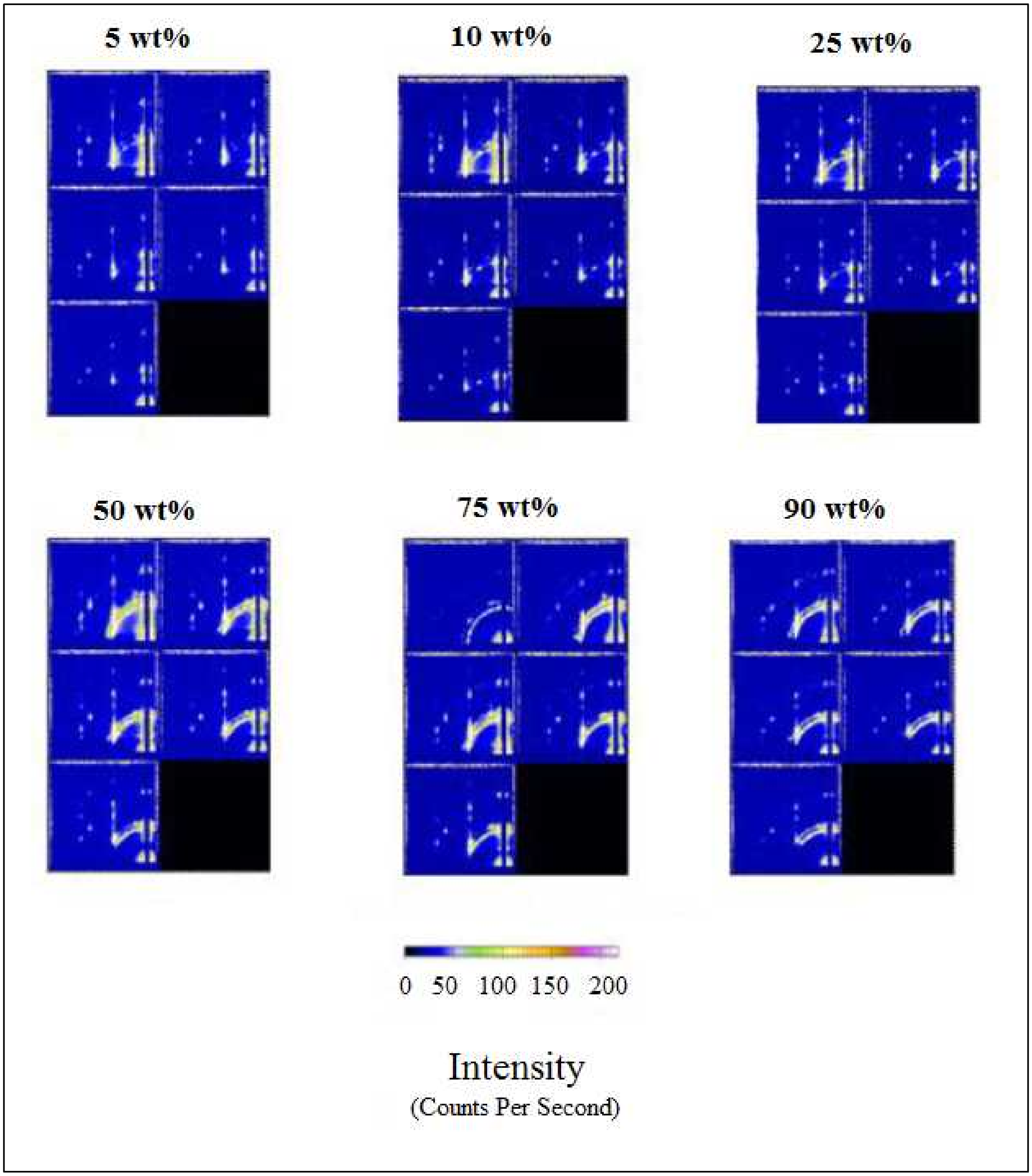

Figure 3.9 - GISAXS spectra of PbS with 820 g mol^{-1} polystyrene at various angles and concentrations (Angles of incidence, labeling clockwise: 0.15°, 0.25°, 0.30°, 0.40°, 0.50°)

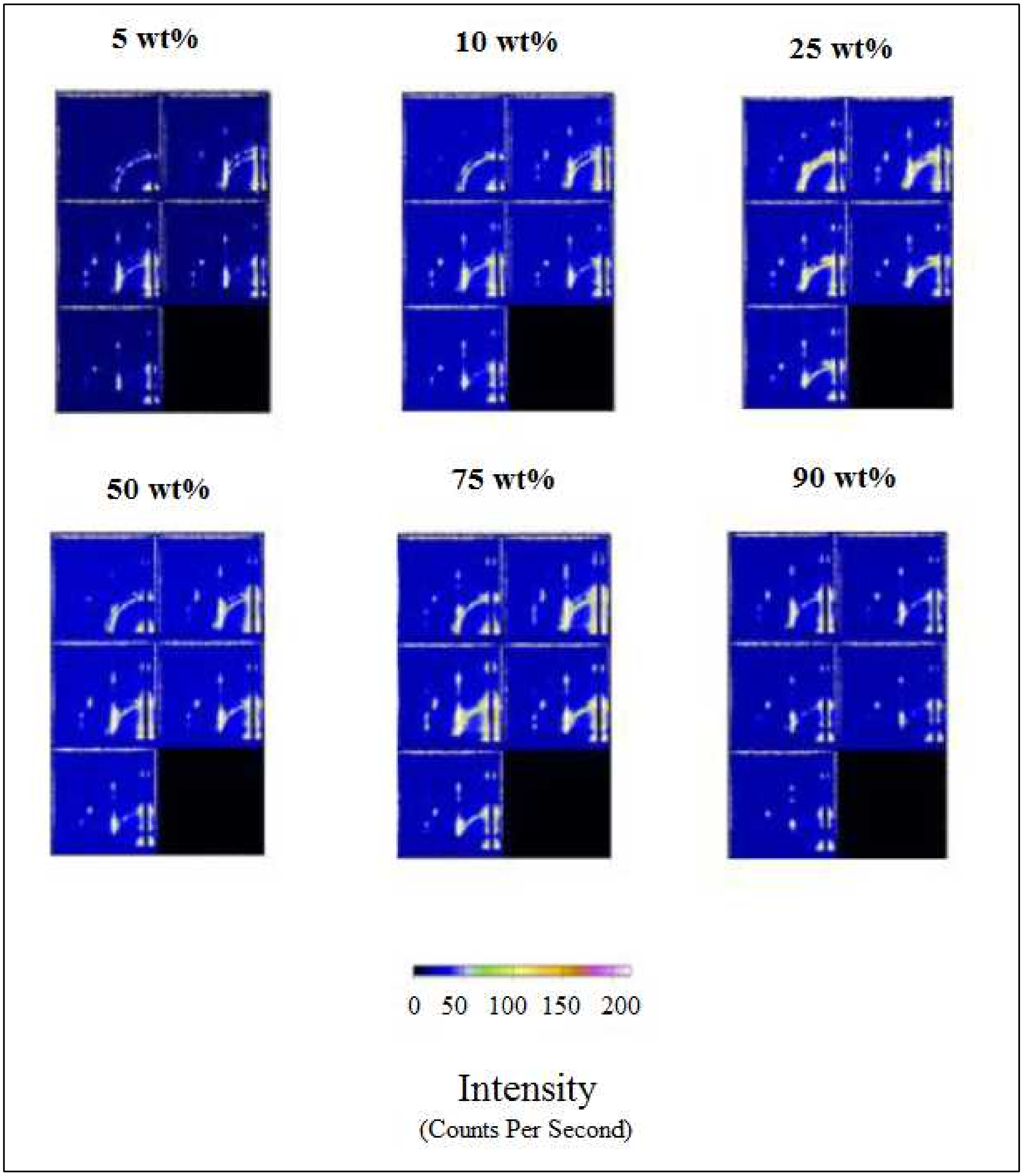

Figure 3.10 - GISAXS spectra of PbS with 18,100 g mol^{-1} polystyrene at various angles and concentrations (Angles of incidence, labeling clockwise: 0.15°, 0.25°, 0.30°, 0.40°, 0.50°)

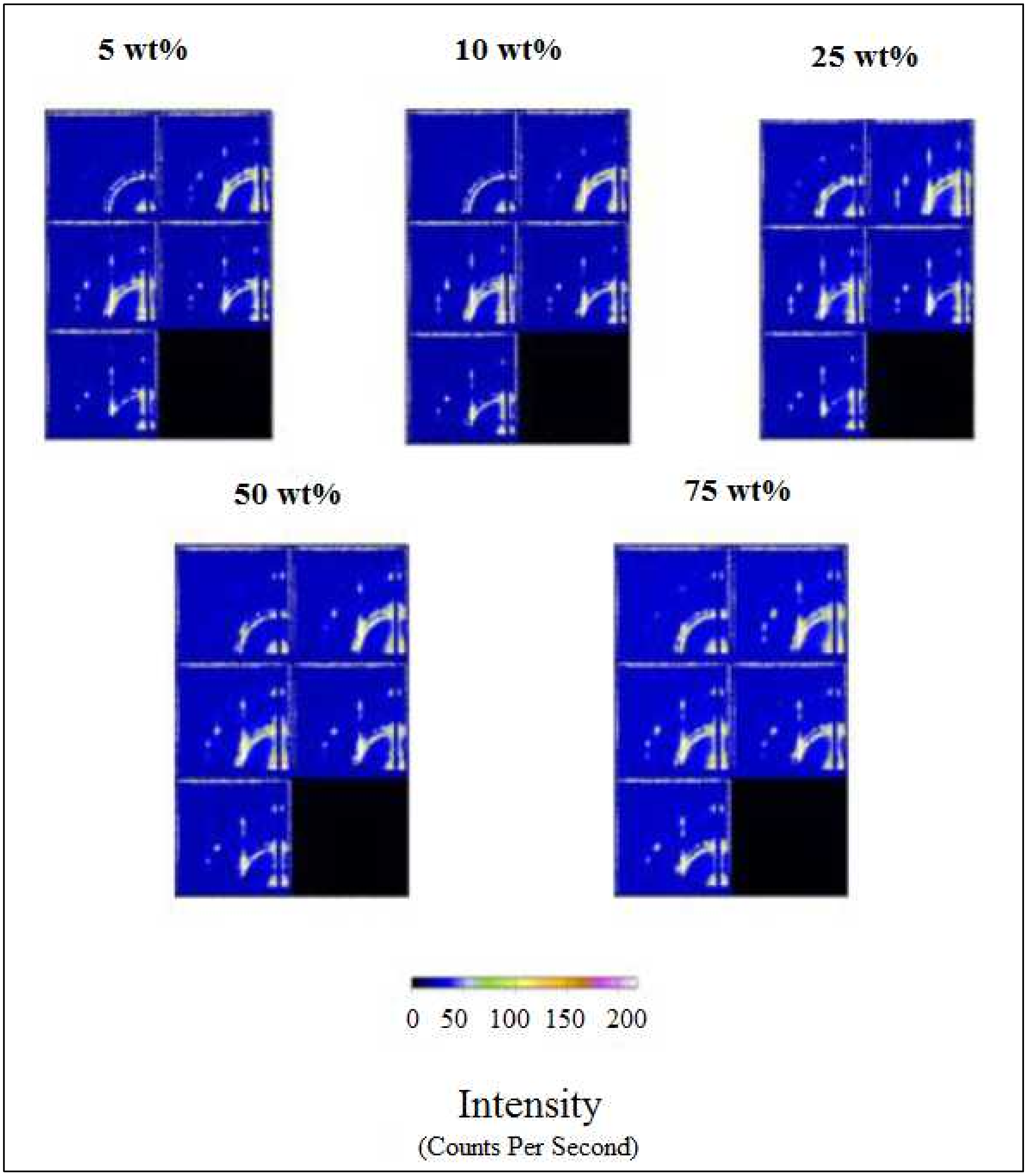

Figure 3.11 - GISAXS spectra of PbS with 97,400 g mol-1 polystyrene at various angles and concentrations (Angles of incidence, labeling clockwise: 0.15^{o}, 0.25^{o}, 0.30^{o}, 0.40^{o}, 0.50^{o})

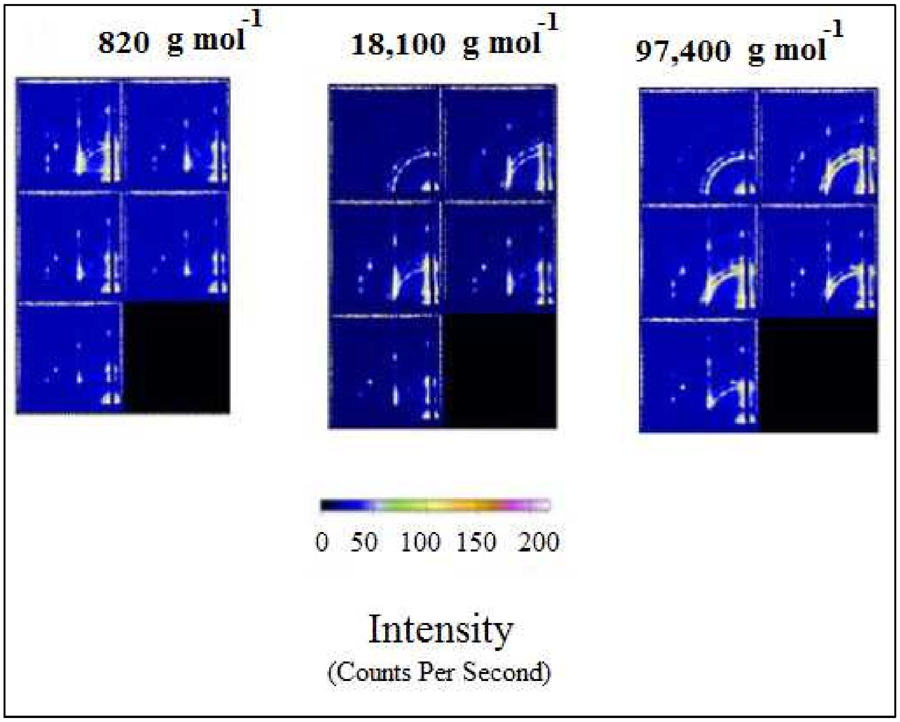

Figure 3.12 - GISAXS Patterns of PbS and 5wt% polystyrenes (Angles of incidence, labeling clockwise: 0.15^o, 0.25^o, 0.30^o, 0.40^o, 0.50^o)

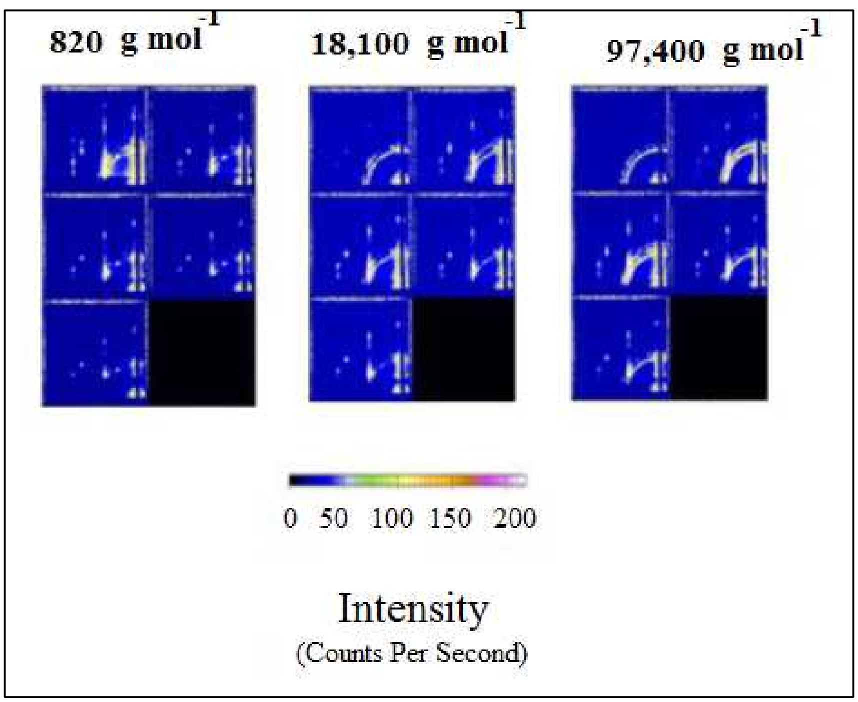

Figure 3.13 - GISAXS Patterns of PbS and 10 wt% polystyrenes (Angles of incidence, labeling clockwise: 0.15^o, 0.25^o, 0.30^o, 0.40^o, 0.50^o)

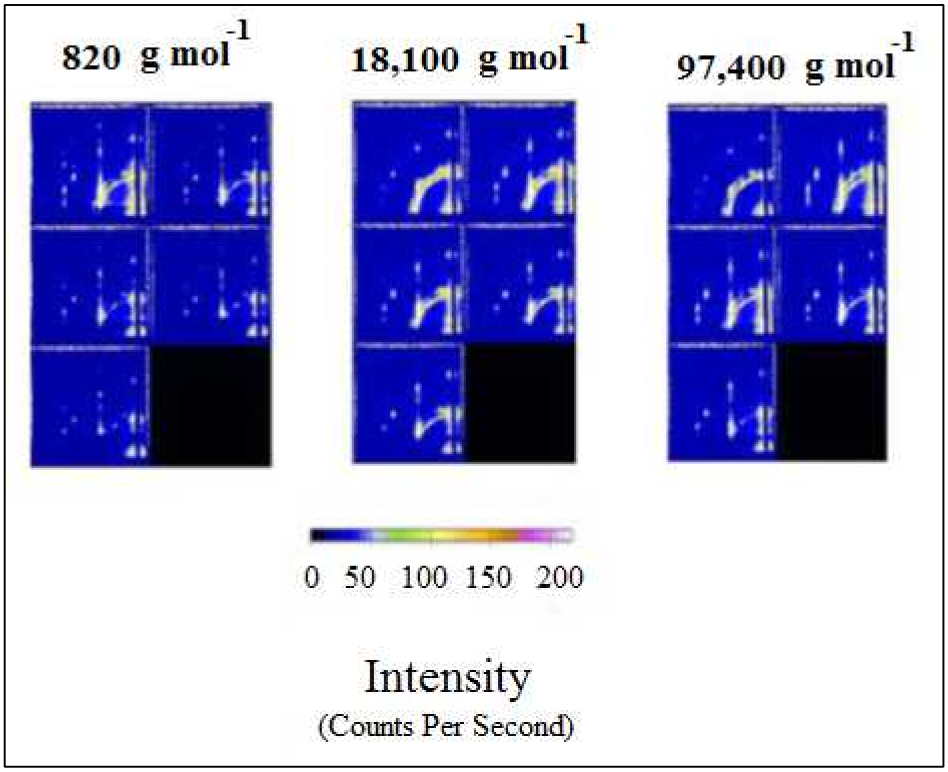

Figure 3.14 - GISAXS Patterns of PbS and 25 wt% polystyrenes (Angles of incidence, labeling clockwise: 0.15°, 0.25°, 0.30°, 0.40°, 0.50°)

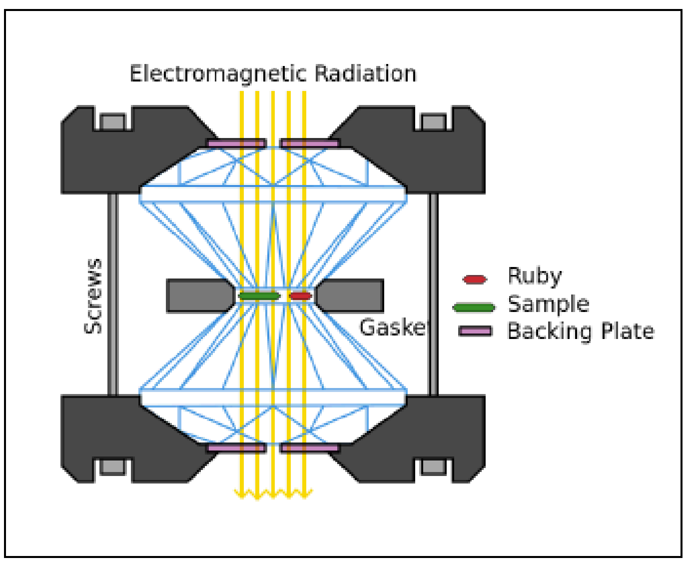

Figure 3.15 - Diamond Anvil Cell construction with sample ruby for calibration (http://en.wikipedia.org/wiki/Diamond_anvil_cell)

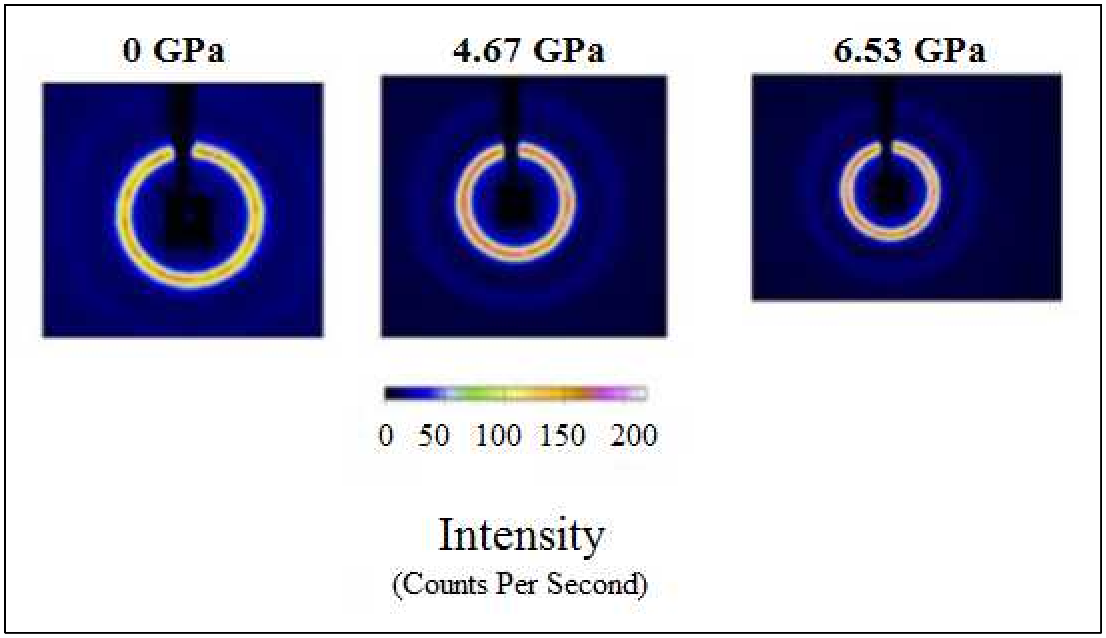

Figure 3.16 - HP-SAXS of Pure PbS film near the threshold pressure (6.90 GPa)

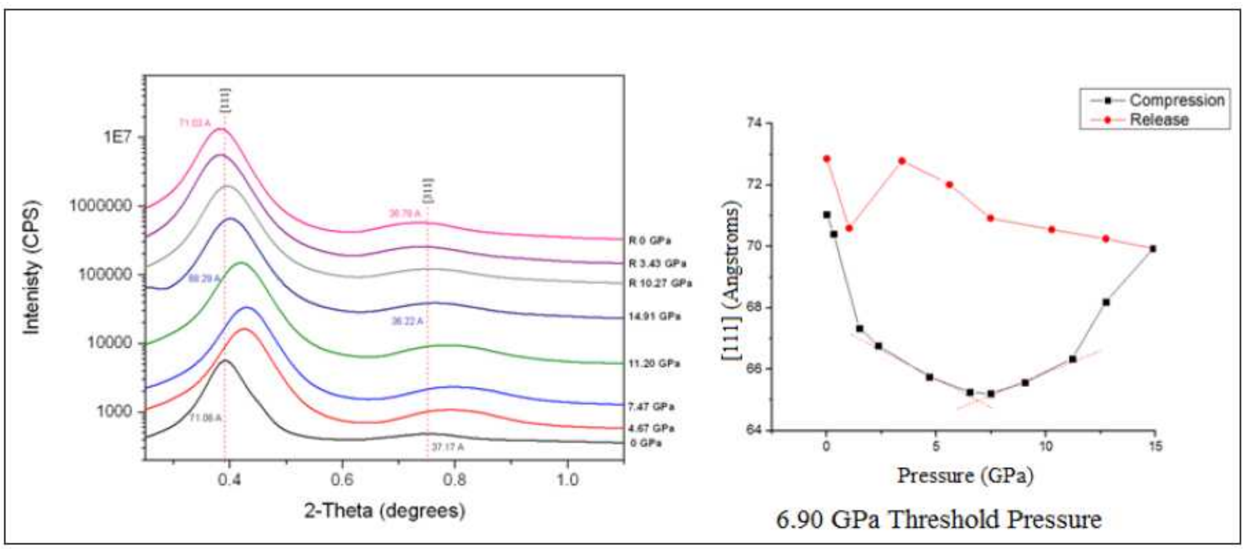

Figure 3.17 - HP-SAXS of Pure PbS and resulting d-spacings

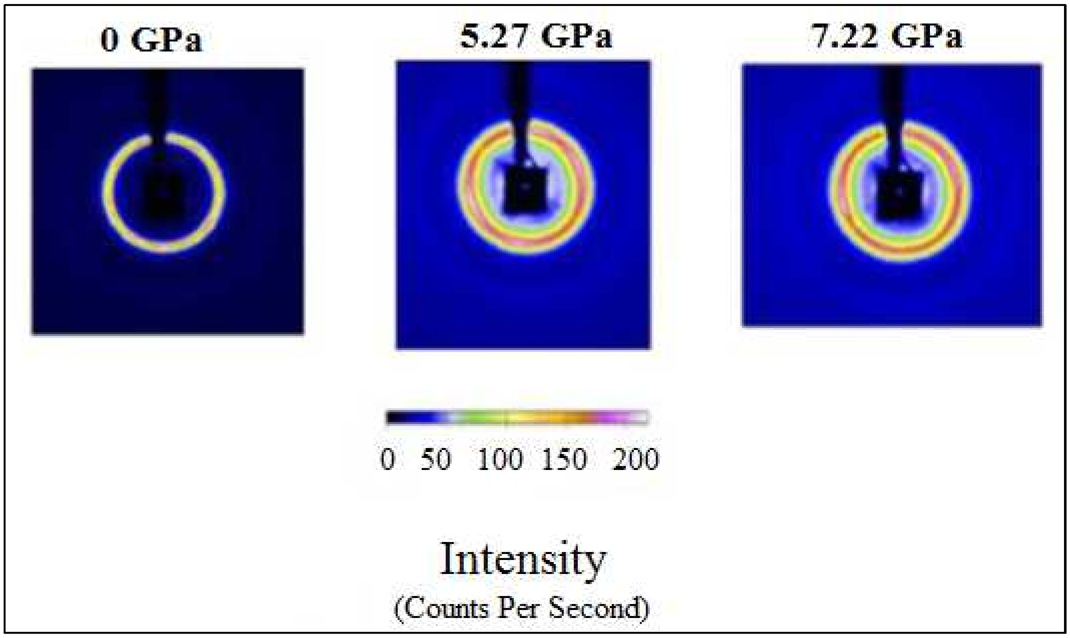

Figure 3.18 - HP-SAXS of PbS 820 g mol^{-1} PS- 25wt% near threshold pressure (6.64GPa)

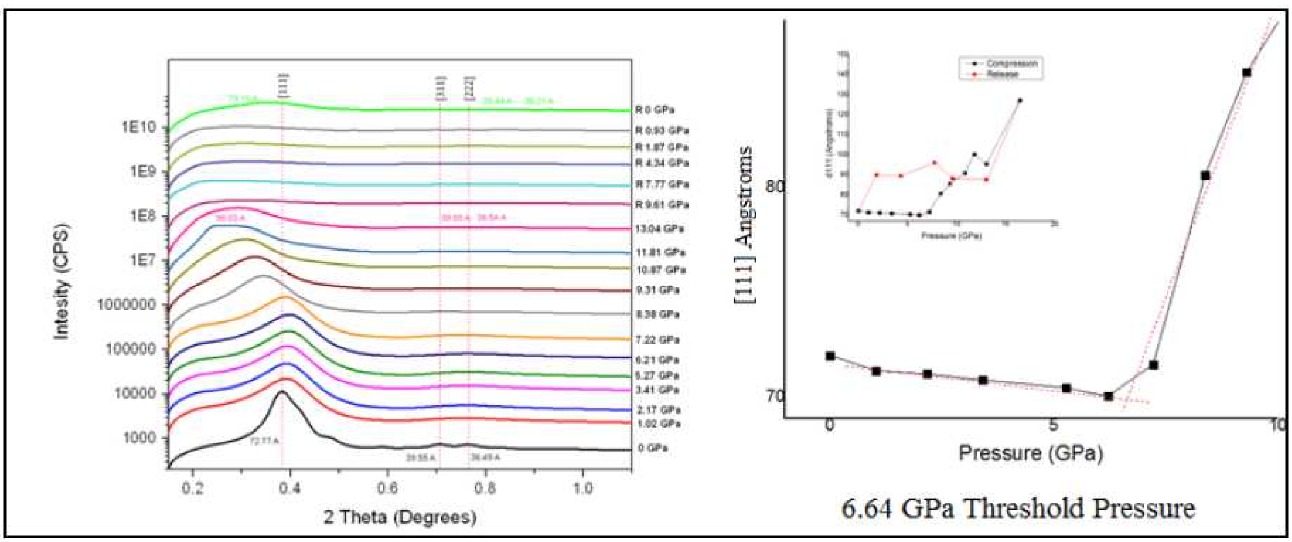

Figure 3.19 - HP-SAXS of PbS-25wt%-820 g mol^{-1} PS and resulting d-spacings

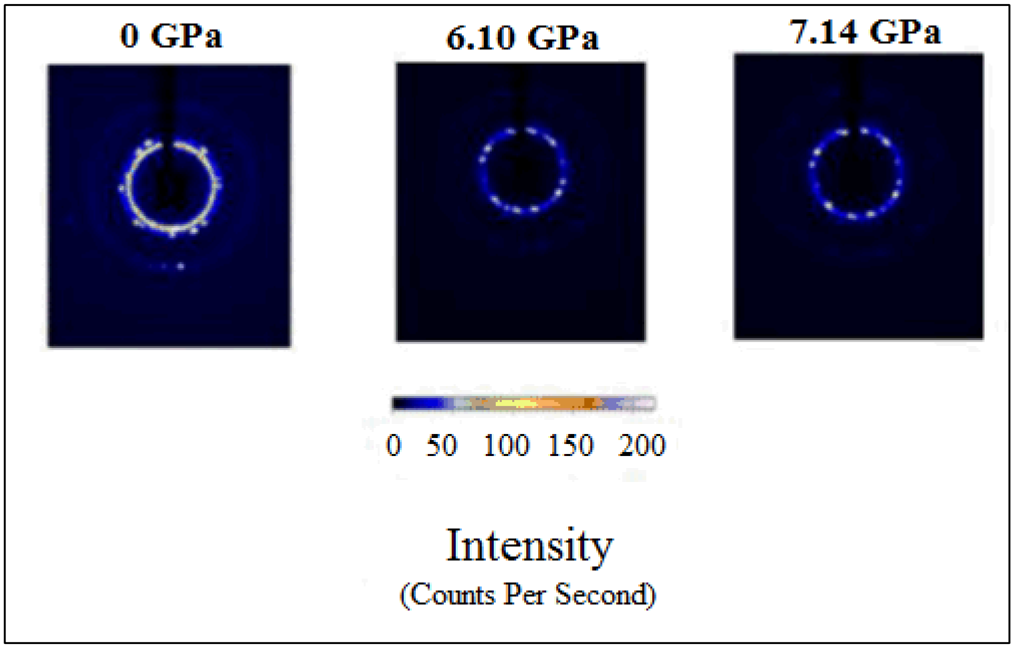

Figure 3.20 - HP-SAXS of PbS-25wt%-18,100 g mol^{-1} polystyrene near threshold pressure (6.20 GPa)

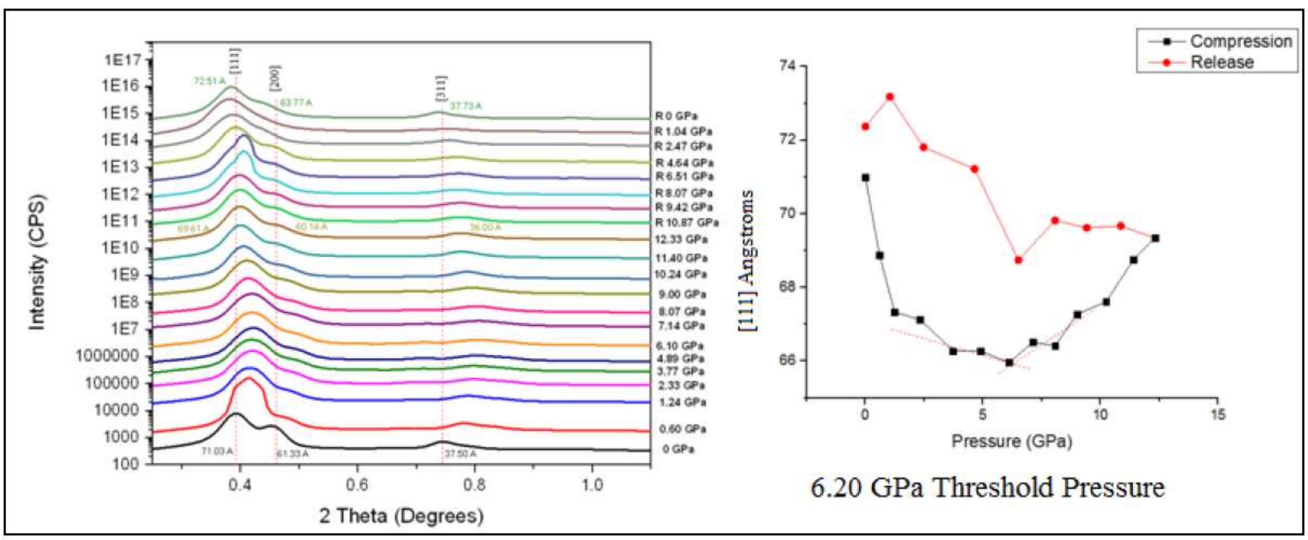

Figure 3.21 - HP-SAXS of PbS-25wt%-18,100 g mol^{-1} PS and resulting d-spacings

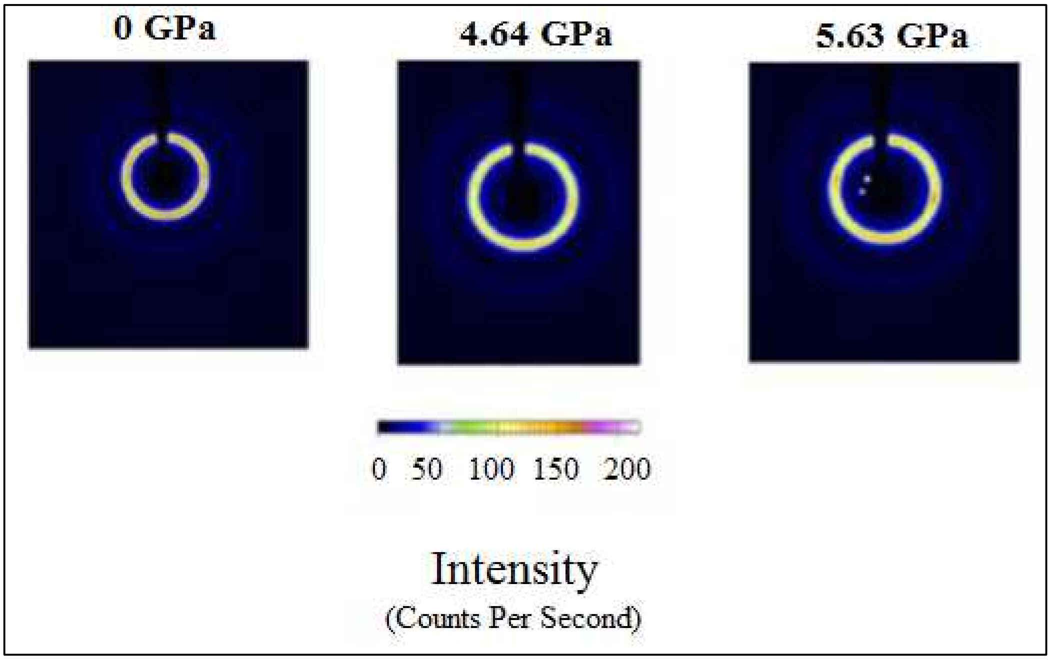

Figure 3.22 - HP-SAXS of PbS-25wt%-97,400 g mol^{-1} polystyrene near threshold pressure (5.58 GPa)

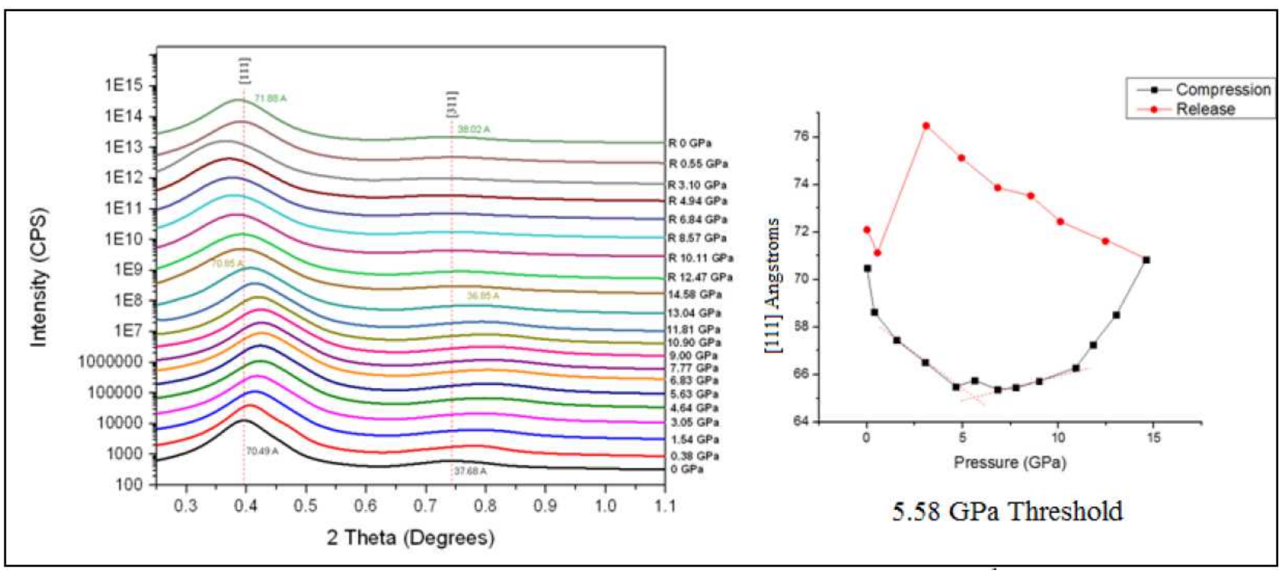

Figure 3.23- HP-SAXS of PbS-25wt%-97,400 g mol^{-1} polystyrene and resulting d-spacings

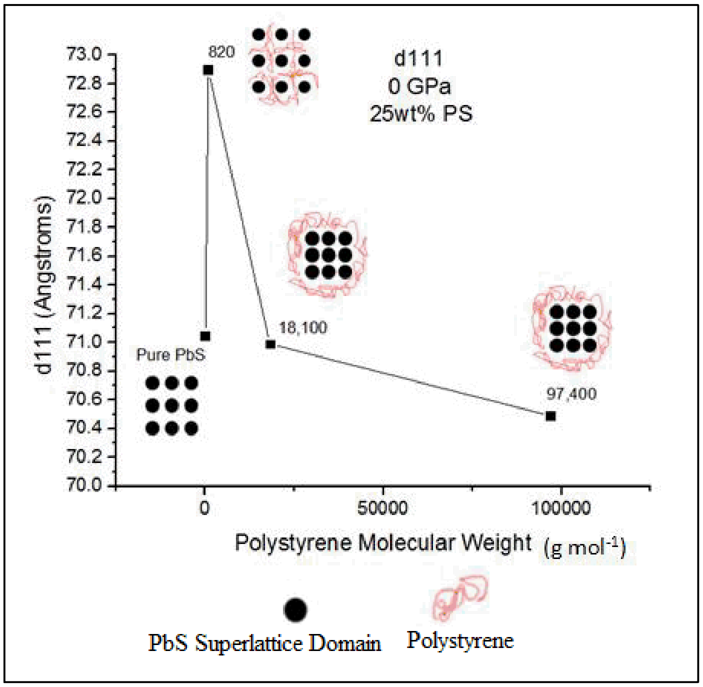

Figure 3.24 - Molecular weight of 25wt% polystyrene versus [111] d-spacing of the composite. Cartoon depicting polystyrene's insertion between or around the superlattice

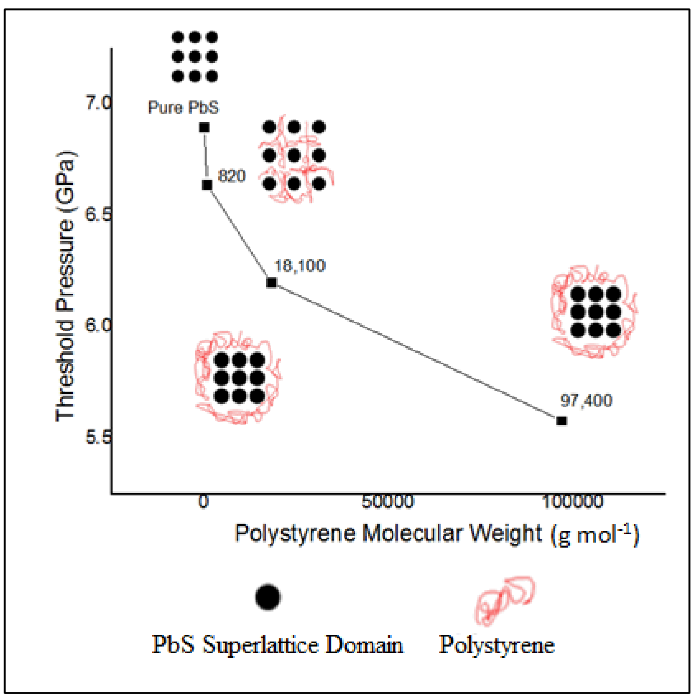

Figure 3.25 - Relationship of 25wt% polystyrene molecular weight to threshold pressure of the composite. Cartoon depicting polystyrene's insertion between or around the superlattice

References

1. Garcia-Santamaria et al., *American Chemical Society Nano*, Vol. 11, **2011**, 687-693

2. Qu, Lianhua. Peng, Xiaogang. *Journal of the American Chemical Society*, Volume 124, Number 9. **2002**. 2049-2055

3. Brus, L.E., *Journal of Physical Chemistry*, 1986. Vol. 90, 2555

4. Ekimov, A. I. & Onushchenko, A. A.. *Journal of Experimental and Theoretical Physics Letters.* 34, **1981**, 345–349

5. R. Rossetti, S. Nakahara, L. E. Brus. *Journal of Chemical Physics.*, **1983**, 79, 1086

6. P. Walter, E. Welcomme, P. Hallegot, N. J. Zaluzec, C. Deeb, J. Castaing, P. Veyssiere, R. Breniaux, J. L. Leveque, G. Tsoucaris. *Nanoletters,* **2006**, *6*, 2215–2219

7. C. B. Murray, C. R. Kagan, and M. G. Bawendi. *Annual Review of Material Science*. 30, **2000**, 545

8. E. Schevenko, D. V. Talapin, C. B. Murray, S. O'Brien *Journal of the American Chemical Society*., 128, **2006**, 3620-3637

9. M. Hines, G. Scholes. *Adv. Mater*. 21, **2003**, 1844-1849

10. J. Akhtar, M. A Malik, P. O'Brien, K. G. U Wijayantha, R. Dharmadasa, S. J. O. Hardman, D. M. Graham, B. F. Spencer, S. K. Stubbs, W. R. Falvell, D. J. Binks, M. El Kazzi, M. Silly. *Journal of Materials Chemistry*, 20, **2010**, 2336-2344

11. J. Joo, H. B. Na, T. Yu, J. H. Yu, Y. W. Kim, F. Wu, J. Zhang, T. Hyeon. *Journal of the American Chemical Society*., 125, **2003**, 11100-11105

12. L. Cademartiri, J. Bertolotti, R. Sapienza, D. Wiersma, G. von Freymann, G. A. Ozin. *Journal of Physical Chemistry B.* 110 Vol. 2, **2006**, 671-673

13. I. Moreels, Y. Justo, B. De Geyter, K. Haustraete, J. Martins, Z. Hens. *American Chemical Society*. Volume 5, Number 3, 2011, 2004-2012 85

14. B. Prasad, S. Stoeva, C. Sorensen, K. Kablunde. *Chemistry of Materials,* **2003**, 15, 935

15. M. Nagel, S. G. Hickey, A. Frömsdorf, A. Kornowski, H. Weller. *Z. Phys. Chem.* 221, **2007**, 427-437

16. L. Bakueva, I. Gorelikov, S. Musikhin, X. Zhao, E. Sargent, E. Kumacheva. *Advanced Materials*, Vol. 16, No. 11, **2004**, 926-929

17. S. Lee, Y. Jun, S. Cho, J. Cheon. *Journal of the American Chemical Society*, **2002**, 124, 11244 – 11245

18. R. Jin, Y. Cao, C. Mirkin, C. Kelly, K. Schatz, J. Zheng, *Science*, **2001**, 294, 1901 C. Schliehe, M. Pelletier, S. Jander, D. Greshnykh, M. Nagel, A. Meyer, S. Foerster, A. Kornowski, C. Klinke, H. Weller. *IMDEA Nanoscience*, 2011

19. K. Yong, Y. Sahoo, M. Swihart, P. Prasad. *Journal of Physical Chemistry*, 125, **2007**, 2447

20.T. Duan, W. Luo, X. Wang, Q. Xue. *Colloids and Surfaces A: Physicochemical and Engineering Aspects*. 310, **2007**, 86-93

21. A. Nejo, A. Nejo, R. Pullabhotla, N. Revaprasadu.. *Journal of Alloys and Compounds*, 537, *2012*, 19-23

22. A. Alivisatos. *Science*. 289. **2000**, 736-737

23. J. Wu, L. Lyu, C. Liao, Y. Wang, M. Huang. *Chemistry: A European Journal*. 18. **2012**, 14473-14478

24. V. Puntes, K. Krishnan, A. Alivasatos. *Science*. 291, **2001**, 2115

25. D. Talapin, C. Murray. *Science* **2005**, 310, 86–89.

26. J. Caruge, J. Halpert, V. Wood, V. Bulovic, M. Bawendi. *Nature Photonics*. **2008**, 2, 247–250.

27. G. Konstantatos, I. Howard, A. Fischer, S. Hoogland, J. Clifford, E. Klem, L. Levina,

28. E. Sargent. *Nature.* **2006**, 442, 180–183. 86

29. P. Podsaidlo, B. Lee, V. Prakapenka, G. Krylova, R. Schaller, A. Demortiere, E. Shevchenko. *Nanoletters*, 11, **2001**, 579-588

30. H. Wu, F. Bai, Z. Sun, R. Haddad, D. Boye, Z. Wang, J. Huang, H. Fan. *Journal of the American Chemical Society*,132, **2010**, 12826-12828.

31. Z. Wang, C. Schliehe, T. Wang, Y. Nagaoka, Y. Cao, W. Basset, H. Wu, H. Fan, H. Weller. *Journal of the American Chemical* Society, 133, **2011**, 14484-14487

32. H. Wu, F. Bai, Z. Sun, R. Haddad, D. Boye, Z. Wang, J. Huang, H. Fan. *Angewandte Chemie International Edition*, 49, **2010**, 8431-8434